Brain Structure and Function (2021) 226:1423–1435
https://doi.org/10.1007/s00429-021-02248-1

ORIGINAL ARTICLE

Connective profiles and antagonism between dynamic and static connectivity underlying generalized epilepsy

Sisi Jiang[1] · Hechun Li[1] · Haonan Pei[1] · Linli Liu[1] · Zhiliang Li[1] · Yan Chen[1] · Xiangkui Li[1] · Qifu Li[2] · Dezhong Yao[1,2,3,4] · Cheng Luo[1,3,4]

Received: 23 June 2020 / Accepted: 27 February 2021 / Published online: 17 March 2021

Abstract

This study aims to characterize the connective profiles and the coupling relationship between dynamic and static functional connectivity (dFC and sFC) in large-scale brain networks in patients with generalized epilepsy (GE). Functional, structural and diffuse MRI data were collected from 83 patients with GE and 106 matched healthy controls (HC). Resting-state BOLD time course was deconvolved to neural time course using a blind hemodynamic deconvolution method. Then, five connective profiles, including the structural connectivity (SC) and BOLD/neural time course-derived sFC/dFC networks, were constructed based on the proposed whole brain atlas. Network-level weighted correlation probability (NWCP) were proposed to evaluate the association between dFC and sFC. Both the BOLD signal and neural time course showed highly concordant findings and the present study emphasized the consistent findings between two functional approaches. The patients with GE showed hypervariability and enhancement of FC, and notably decreased SC in the subcortical network. Besides, increased dFC, weaker anatomic links, and complex alterations of sFC were observed in the default mode network of GE. Moreover, significantly increased SC and predominantly increased sFC were found in the frontoparietal network. Remarkably, antagonism between dFC and sFC was observed in large-scale networks in HC, while patients with GE showed significantly decreased antagonism in core epileptic networks. In sum, our study revealed distinct connective profiles in different epileptic networks and provided new clues to the brain network mechanism of epilepsy from the perspective of antagonism between dynamic and static functional connectivity.

Keywords Structural connectivity · Functional connectivity · Static · Dynamic · Epilepsy

Introduction

Epilepsy is a neurological disorder characterized by abnormally synchronous activity of a large number of neurons in the brain. The generalized epilepsy (GE) has been recognized as a network disorder involving distributed regions in a large-scale brain network. Specifically, the thalamocortical network has been identified to be a crucial circuit for epileptic activities in GE (Gotman et al. 2005; Jiang et al. 2018). Large-scale functional network analysis in epilepsy has provided valuable information on seizure generation, propagation and termination (Ponten et al. 2007; Kramer et al. 2008; Schindler et al. 2008). Disrupted complex structural connectivity (SC) network was suggested to serve as anatomical evidence to support the functional abnormalities in patients with GE (Xue et al. 2014). Notably, deceased function–structure coupling of large-scale brain networks has been viewed to reflect the long-term impairment of brain

✉ Cheng Luo
Chengluo@uestc.edu.cn

1 The Clinical Hospital of Chengdu Brain Science Institute, MOE Key Lab for Neuroinformation, School of Life Science and Technology, University of Electronic Science and Technology of China, Qingshuihe Campus: No.2006, Xiyuan Ave, West Hi-Tech Zone, Chengdu 611731, People's Republic of China

2 Department of Neurology, First Affiliated Hospital of Hainan Medical University, Haikou, China

3 Research Unit of NeuroInformation, Chinese Academy of Medical Sciences, 2019RU035, Chengdu, China

4 High-Field Magnetic Resonance Brain Imaging Key Laboratory of Sichuan Province, Center for Information in Medicine, University of Electronic Science and Technology of China, Chengdu, People's Republic of China

in GE (Zhang et al. 2011). In recent years, accumulated studies have suggested a possibility that dynamics of functional connectivity (FC) could be a hot candidate for a biomarker in neuropsychiatric disorders, such as schizophrenia (Sakoglu et al. 2010) and Alzheimer's disease (Rubinov and Sporns 2011). Moreover, accumulated dynamic FC (dFC) researches in epilepsy have also been conducted. Liao et al. revealed abnormally changed dFC between resting-state networks in patients with idiopathic generalized epilepsy and suggested that the features derived from dynamic functional network connectivity (dFNC) analysis could be potential biomarkers to distinguish patients from controls with a high accuracy (Liu et al. 2017). In all, disrupted static FC (sFC), SC and dFC have been demonstrated in epilepsy provided important evidences to understand the pathomechanism of epilepsy.

The synchronization of spontaneous neuronal activity of different brain regions is known as functional connectivity (FC) (Biswal et al. 1995; Lowe et al. 2000), which captures the temporal correlations or statistical dependences between brain regions (Sporns et al. 2004). Structural connectivity (SC) is sustained by a set of white matter pathway linking neuronal units of our brain (Sporns et al. 2004) and can be macroscopically estimated using diffusion tensor imaging (DTI) (Mori and van Zijl 2002). It has been recognized that the SC shapes the diverse patterns of FC and the FC reflects the SC architecture of cerebrum (Wang et al. 2015). The main divergences and discrepancies between SC and FC come from the high flexibility of FC and relative fixation of SC (Allen et al. 2014; Chang and Glover 2010). Brain regions dynamically integrate, segregate and coordinate in different brain states to respond to internal and external stimuli. Dynamic FC (dFC) quantifies changes of sFC over time and reflects flexibility and variability of information interaction between brain regions. Emerging evidence has suggested that dFC reveals neural activity patterns associated with changes in cognition and behavior (Hutchison et al. 2013a). However, up to now, it is less studied about the association between dFC and sFC in a large-scale brain network level. The question of how dFC and sFC associate with each other is of considerable theoretical importance. And we further propose that investigation of the underlying relationship between dFC and sFC in epilepsy might provide distinctive clues from a novel aspect to reveal pathological features of epileptic brain network.

This study first aims to investigate the SC, dFC and sFC alterations in large-scale networks in GE. Second, the present work seeks to study the association between dFC and sFC and its potential in investigating epileptic brain. Notably, a recent study indicated that HRF variability significantly affects resting-state FC calculation and suggested a neural FC to reduce false positive/negative connectivity (Rangaprakash et al. 2018b). The present study will perform dFC and sFC using both BOLD and neural time course, trying to provide more reliable results.

Materials and methods

Participants

Eight-three patients (mean age: 22.59 ± 11.18 years; mean years of duration: 7.75 ± 8.36; mean age of seizure onset: 14.84 ± 10.86; all right-handed, 39 males) with GE were recruited in the present study. All the patients underwent a comprehensive clinical evaluation for the diagnosis of GE according to the epilepsy classification of the International League Against Epilepsy (Engel and International League Against 2001). Detailed demographic and clinical information are shown in Table 1. No patients had brain lesions, developmental disabilities, or other accompanying neurological disorders. One hundred and six healthy controls (mean age: 23.57 ± 10.42 years, all right-handed, 60 males) were recruited as a sex- and age-matched control group, and all the controls were free from neurological and psychiatric disorders. This study was approved by the ethical committee of the University of Electronic Science and Technology of China according to the standards of the Declaration of Helsinki, and written informed consent was obtained from each subject and their parents.

Data acquisition

All subjects underwent MRI scanning in a 3T GE scanner with an eight-channel-phased array head coil (EXCITE, GE, Milwaukee, WI) in the Affiliated Hospital of the North Sichuan Medical College. Resting-state functional data were collected using an echo-planar imaging sequence with the following parameters: repetition time (TR) = 2000 ms, echo time (TE) = 30 ms, flip angle (FA) = 90°, slice

Table 1 Clinical characteristics in GE and HC

Characteristic	GE	HC	*p* value
Number	83	106	–
Age (year)	22.6 ± 11.2	23.6 ± 10.4	0.54[a]
Gender (F:M)	39:44	46:60	0.62[b]
AED (with:without)	66:15	–	–
Therapy (single:multiple)	26:40	–	–
Age at onset (year)	14.8 ± 10.9	–	–
Duration (year)	7.7 ± 8.4	–	–
mFD	0.12 ± 0.06	0.08 ± 0.03	< 0.001[a]

AED: antiepileptic drug; mFD: mean frame-wise displacement

[a]The *p* value was obtained by a two-sample two-tail t test

[b]The *p* value was obtained by a χ^2 test

thickness = 4 mm (no gap), data matrix = 64 × 64, field of view = 24 cm × 24 cm, voxel size = 3.75 × 3.75 × 4 mm^3, and 32 axial slices in each volume. Two hundred and fifty-five volumes were acquired in each scan. All subjects were instructed to close their eyes and relax without falling asleep during the scan. Axial anatomical T1-weighted images were acquired using a three-dimensional fast spoiled gradient echo sequence. The parameters were as follows: thickness = 1 mm (no gap), TR = 8.2 ms, TE = 3.2 ms, field of view = 25.6 cm × 25.6 cm, flip angle = 12°, data matrix = 256 × 256. There were 136 axial slices for each subject. The diffusion tensor image (DTI) data were acquired using a single-shot, spin-echo, echo-planar sequence (75 slices, voxel size 2 × 2 × 2 mm^3, 128 × 128 base resolution, diffusion weighting isotopically distributed along 64 directions, *b* value 1000 s/mm^2).

Network construction

The nodes of the brain connectivity network were determined using a brain atlas proposed by Jiang's Group (Fan et al. 2016), which segments whole cerebrum into 246 anatomical regions of interest (ROI, 123 regions for each hemisphere). Both the functional and structural connectivity networks were constructed based on the atlas, generating a 246*246 connectivity matrix for each participant. Figure 1 illustrates the construction of anatomical, static and dynamic functional connectivity networks and the further coupling analysis.

Structural connectivity network construction

In the present study, Diffusion Toolkit (www.trackvis.org/dtk/) was used to preprocess DTI data. First, non-brain tissues were eliminated from DTI data using the brain extraction tool (BET) of the FSL. For each subject, 64 diffusion-weighted images were registered to a non-diffusion-weighted average B0 image ($b = 0$ s/mm^2) using affine transformations to correct head movements. To estimate the susceptibility-induced distortions, two types of images were acquired using R/L and A/P frequency directions without any diffusion weighting, which was introduced to the FSL topup tool. Then, the effects of distortion induced by eddy currents, inter-volume movements and the susceptibility of the diffusion data were corrected using eddy. Linear least-squares fitting method was used to estimate diffusion tensor models in every voxel using the Diffusion Toolkit.

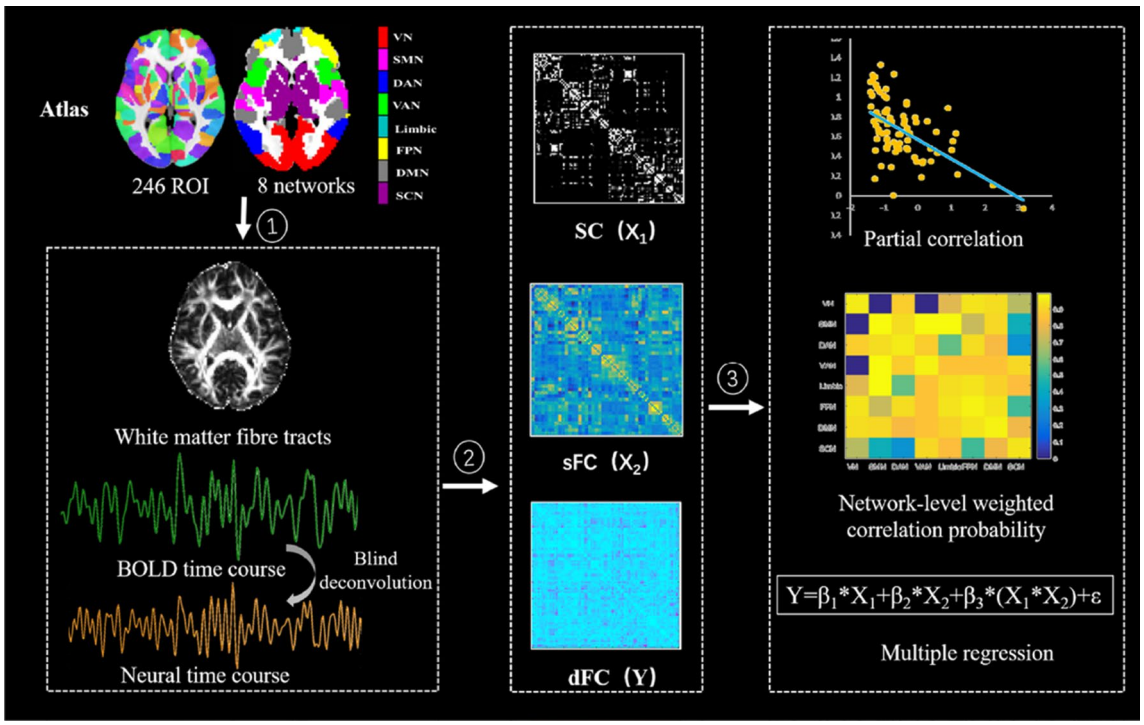

Fig. 1 Illustration of anatomical, static, and dynamic functional connectivity networks construction and coupling analyses. (1) The 246 nodes of network are based on a propose atlas. The BOLD time course of each sub-regions was extracted and further deconvolved into neural activity. (2) The SC connections are defined by the total number of streamlines between the two nodes, the sFC weights was measured by Pearson's r coefficients and the dFC index was computed using sliding-window approach (window length = 50 TR and step = 1 TR). (3) Coupling analysis was performed using partial correlation and multiple linear regression methods. An indicator named NWCP was computed to investigate the coupling relationship at the network level

Before constructing structural connectivity network, 246 nodes of network were defined in native diffusion space based on a human brainnetome atlas (Fan et al. 2016). Specifically, a warp image was generated by first co-registering individual T1-weighted image to diffusion B0 image and then mapped to the ICBM-152 MNI T1-template. The ROI template in MNI space was warped to individual DTI native space using the inverted warp image. Then, for each subject, deterministic tractography was performed in the native diffusion space to construct whole-brain SC network using the Fiber Assignment by Continuous Tracking (FACT) algorithm embedded in the Diffusion Toolkit. When reaching a voxel with fractional anisotropy < 0.15 or/and contiguous path segment exceeded 35°, the path tracing would stop. The connectivity strength between two nodes was measured by the total number of streamlines connecting them. To reduce false connectivity, any two nodes with less than three streamlines between them were considered to have no connection. Finally, a symmetric and weighted 246*246 SC matrix was generated for each subject.

Besides, a structure-restricted connection mask was generated. Specifically, in each individual, any edges less than three connections were set to zero. Then, only the edges existed in more than 80% subjects were preserved in the group-level SC mask. The SC mask was used to restrict following sFC and dFC matrix.

Functional connectivity network construction

Resting-state fMRI data were preprocessed using the NIT software package (http://www.neuro.uestc.edu.cn/NIT.html). The first five volumes were discarded to ensure magnetic field stabilization. The remaining 250 volumes were slice-timing corrected and spatially realigned. Then, the functional data were spatially normalized to the standard Montreal Neurological Institute space and were resampled to 3 mm × 3 mm × 3 mm and smoothed with a Gaussian kernel (8 mm full width at half maximum, FWHM). Finally, the linear trend signals, the whole brain mean signal, and white matter and cerebrospinal fluid signals were regressed out from the smoothed resting-state fMRI data. Any subject whose head motion exceeded 2 mm or/or 2° was excluded. Given the potential influence of head-motion on connectivity analysis, 24 head-motion parameters were regressed out from the preprocessing images. We performed a band pass filter of 0.01–0.1 Hz for the time series in the present study. Additional, mean frame displacement (mFD) was calculated for every subject and considered as a nuisance in the statistical general linear model. The mFD has been recognized as a robust index to measure head-motion, which can be calculated by the following equation (Power et al. 2012):

$$\mathrm{mFD} = \left(\frac{1}{M-1}\right)\sum_{i=2}^{M}(|\Delta d_{x_i^1}| + |\Delta d_{y_i^1}| + |\Delta d_{z_i^1}| + |\Delta d_{x_i^2}| + |\Delta d_{y_i^2}| + |\Delta d_{z_i^2}|),$$

where M is the length of the time course; x_i^1/x_i^2, y_i^1/y_i^2 and z_i^1/z_i^2 are translations/rotations at the ith time point in the x, y, and z directions, respectively; and $\Delta d_{x_i^1} = x_i^1 - x_{i-1}^1$, and a similar pattern held for the others. Notably, by calculating displacement on the surface of a sphere with a radius of 50 mm, the rotations were converted from degrees to millimeters.

Representative BOLD time course in each ROI was extracted by averaging the functional time series across all voxels in this region. The neural time course was estimated using a blind deconvolution approach (Wu et al. 2013), which modeled the resting-state BOLD time course as event-related response with randomly occurring events (Tagliazucchi et al. 2012). More detailed description about the blind deconvolution is presented in the supplementary materials. This approach is widely accepted and has been applied in many published works (Rangaprakash et al. 2017a, b, 2018a). Then, both the BOLD and neural time course were used for constructing functional connectivity network with same process as following. Pairwise correlations in 246 brain regions was calculated using Pearson correlation coefficients, generating a 246*246 static connectivity matrix (no duplicate 30,135 edges) for each subject. A Fisher-Z transformation was applied to all Pearson correlation coefficient matrix to improve the normality of the correlation distribution.

The construction of dFC network was computed using a sliding-window correlation method. A 100 s window length ($L = 50\ TR$) and a step of 2 s ($S = 1\ TR$) were used, considering that the window length should be in line with the commonly identified slowest frequency of the BOLD signal (Leonardi and Van De Ville 2015; Zalesky and Breakspear 2015). Briefly, for a given voxel, the time series, consisting of 250 time points ($F = 250\ TR$), was segmented at each time point by obtaining $201\ (W = F - L + 1)$ sequential time windows. The functional connectivity matrix was calculated within each segmented window, thus generating 201 functional connectivity matrices. Then, the standard deviation (SD) across 201 continuous connectivity matrices was calculated to represent the temporal variability of functional connectivity. Finally, the SD matrix was z-standardized across all the 30,135 edges for the following statistical analysis.

Notably, to validate the dynamics of FC captured in the present approach, as suggested previously (Hutchison et al. 2013a; Hindriks et al. 2016), an additional phase randomization analysis was conducted in the HC group. To test whether the observed dFC exhibits significantly greater temporal variability than simple variability around static FC, we

calculated the dFC using phase shuffled surrogate fMRI time series in HC group and compared to the observed variability. Detailed calculation procedure are as follows. (1) For a given region, let $x1, x1, \ldots, xn$ be the time series of n sliding windows. Discrete Fourier transformations $X1$, $X2, \ldots$, Xn are calculated. (2) Multiply the signal's Fourier transform with a random phase $\tilde{X}n = X\_n$ e^($i\varphi\_n$) where φ_1, …, φ_n is a vector of independent stochastic variables that are uniformly distributed in the interval [0, 2π]. (3) Perform inverse discrete Fourier transformation to $\tilde{X}$n to yield randomized $\tilde{X}$ of X. Notably, to preserve the static correlation structure, the same phase randomization process was performed for all regions. (4) Calculate dFC using the phase-random surrogate time series. Further comparisons between the variability in the observed and phase-random datasets was performed using rank-sum tests.

Before following coupling and statistical analyses, all the sFC and dFC matrixes were masked using above SC mask, that is, only the edges in the SC mask defined before were analyzed.

Coupling analysis between dynamic and static FC

Partial correlation calculation was performed between sFC and dFC with age and gender as covariates in HC and GE, respectively. According to the network definition of Yeo et al. and template parcellation of Jiang et al. (Yeo et al. 2011; Fan et al. 2016), 246 nodes were divided into 8 brain networks. Notably, Jiang divided 246 nodes to 7 networks of Yeo and 1 unnamed network, which was named subcortical network (SCN) in the present study. The seven networks include visual network (VN), sensorimotor network (SMN), dorsal attention network (DAN), ventral attention network (VAN), Limbic network (Limbic), frontoparietal network (FPN), and default mode network (DMN). Then, network-level weighted correlation probability (NWCP) was calculated, which was defined by the following formula:

$$\mathrm{NWCP}_{ij} = \frac{\sum_{\substack{m\in N_i \\ n\in N_j}} C_{sig_{m,n}}}{\sum_{\substack{m\in N_i \\ n\in N_j}} C_{m,n}}$$

where N_i, N_j correspond to *ith* and node *jth* network according to Yeo, and m, n is the node in certain network. The $C_{m,n}$ represents the partial coefficients between the sFC and dFC between node m and node n, and C_{sig} is the partial coefficients which is significant ($p < 0.05$). If $i = j$, the NWCP measures the within-network probability, else, is between-network probability. Higher the NWCP implies a higher probability of association between sFC and dFC within or between networks.

Furthermore, the present study wonders to demonstrate the potential effects of anatomic link on the association between sFC and dFC. Thus, we constructed a general linear model (GLM) with the dFC as the dependent variable, the sFC as the independent variable, and the SC and the interaction of SC and sFC as nuisances. The interaction is simply expressed by product of sFC and SC. Notably, both the SC and interaction variables were z-scored. The regression coefficient of sFC reflects the association between static and dynamic FC under a condition ruling out the anatomic support.

Statistical analysis

Structural connectivity statistics

The between-group difference of SC was investigated using the FSL software randomise, which is a non-parametric permutation test based on the modeling and inference using standard GLM design (Winkler et al. 2014). The patients with epilepsy tend to show different levels of abnormalities in multimodal neuroimaging analyses. Specifically, epilepsy is a neurological disease characterized by significant functional damage with relatively slight structural disturbance. The differences of SC were detected using a relatively lenient p-threshold ($p < 0.005$). Considering the relative loose statistic threshold of the SC, to test the reliability of the alteration of SC in GE, we employed another classical brain atlas (AAL) with 90 cerebral sub-regions.

Functional connectivity statistics

The between-group comparisons of the sFC and dFC were performed using the two-sample t test. The $p < 0.001$ was viewed to be significant for the in between-group comparisons with a network-level correction by a family wise error (FWE $p < 0.05$) using 1000 times of permutation. The detailed process of the network-level correction is presented in the supplementary materials. Additionally, significantly altered SC, sFC, and dFC measures in patients were correlated with their clinical characteristics (disease duration and onset of age) with the gender as a nuisance covariate.

The between-group comparison of NWCP was investigated using a permutation test. Specifically, each subject was randomly assigned to one of two random groups in per permutation and kept same number of subjects as the original GE or HC group. Then, difference of NWCP between two random groups was calculated with 1000 permutations, generating a null distribution of between-group difference. Finally, p values were calculated as the proportion of the NWCP values from 1000 permutations that are no less than the original NWCP values. The significant level for the NWCP was set to $p < 0.001$ with FDR correction.

In the coupling analysis using GLM, a rigorous procedure was adopted to identify the significant coupling effect using

the following three criteria: (1) the significant estimation of the GLM with an F test $p < 0.005$, (2) the goodness of fit depicted by a coefficient of determination $R^2 > 0.4$, and (3) the p value of regression coefficient of sFC less than 0.05.

Results

Alterations of streamlines-defined SC

In the present study, altered anatomic connections were observed in the patients with GE compared with HC ($p < 0.005$, uncorrected) (Fig. 2). Predominantly increased SC was found in SCN-related connections in patients with GE, including the SC within SCN and the connections between SCN and DAN, Limbic, FPN and DMN. Decreased within-network SC mainly occurred within VN and SMN, and between-network connections were found in DMN–VN, DMN–SMN, and SCN–Limbic.

Alterations of sFC and dFC

In general, the sFC and dFC derived from BOLD and neural time course demonstrated highly concordant between-group differences ($p < 0.05$ FWE corrected). Thus, following results illustration mainly focused on commonly revealed alterations, ignoring certain edges only occurred in BOLD or neural calculation. Specifically, for the sFC, decreased sFC between SCN and DAN was remarkably observed in GE (Fig. 3). Decreased sFC within VAN, DAN and SMN, and increased sFC within VN were also found. Besides, increased sFC between networks were observed in SMN-DMN, SMN-DNA and SMN-VN. The DMN demonstrate both decreased and increased sFC (Fig. 3).

In the validation analysis using phase random approach, the observed variability was found to be significantly higher than the variability in the phase-random dataset

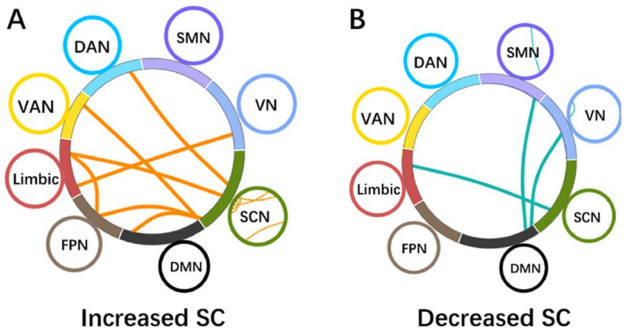

Fig. 2 Disturbed SC in patients with GE. Significant alterations were observed in SCN- and DMN-related connections. The lines with light orange color represent increased connections (**a**) and the blue lines represent decreased connections (**b**)

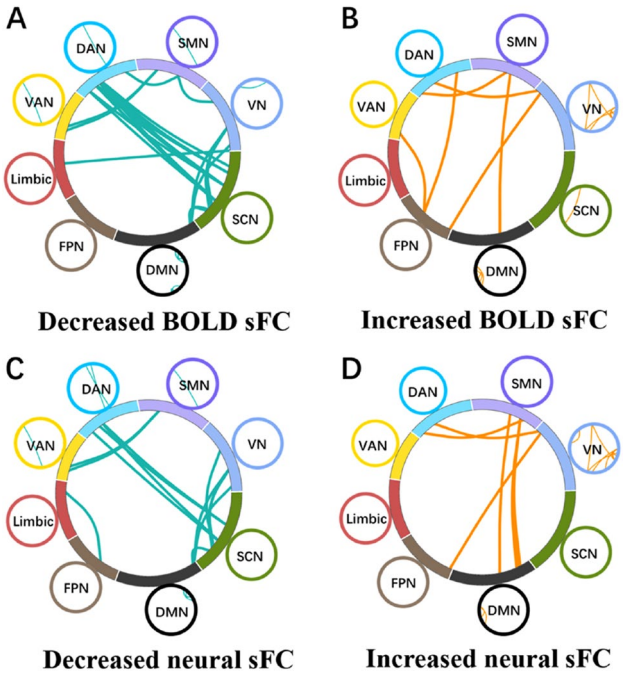

Fig. 3 Altered sFC in patients with GE. The sFC alterations were detected using BOLD (**a** and **b**) and neural time course (**c** and **d**)-derived approaches. The lines with light orange color represent increased connections and the blue lines represent decreased connections. To better convey the main results to a clear extent and keep the core findings unchanged, a stricter statistical threshold $p < 0.05$ corrected with family wise error (FWE) for the sFC was adopted to show the results

($p < 0.05$, FDR corrected). These findings demonstrates that the observed variability is reliable (Fig. S1). For the between-group comparisons of dFC, an uncorrected threshold $p < 0.001$ was adopted in the present study (Fig. 4). Decreased dFC was found within FPN, within VN and between FPN and DAN. Increased dFC was also observed within DMN and SMN in patients. Besides, increased dFC of between-network connections were observed in Limbic-SCN, DMN-VN and VAN-SMN.

The correlation analysis revealed significant association between the connective profiles and clinical features (as illustrated in the Supplementary material, Fig. S2, S3).

Coupling relationship between sFC and dFC

Both the BOLD and neural correlation analyses revealed predominately negative correlation between dFC and sFC in most of the SC-restricted connections in HC and GE group, which implied that the antagonistic relationship might be a generalized phenomenon between dFC and sFC. And, few connections showed positive correlation (Supplementary material, Fig. S4), thus following NMCP analysis only focused on connections with negative correlation values.

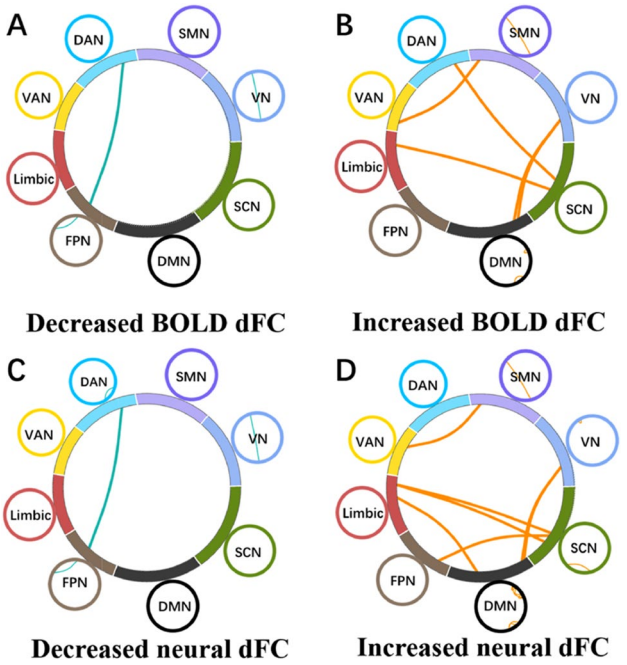

Fig. 4 Altered dFC in patients with GE. The dFC alterations were detected using BOLD (**a** and **b**) and neural time course (**c** and **d**)-derived approaches. The lines with light orange color represent increased connections and the blue lines represent decreased connections

As shown in Fig. 5, all within-network NWCP values reached very high probability (high than 80%). The NWCP in VN-SMN and VN-VAN was zero, which means that the dFC of connections between VN and SMN, VAN is totally not negative with sFC. Besides, the SCN showed weak NMCP with SMN, DAN, FPN, and DMN. The remaining between-group NWCP values were remarkably high in both groups.

Further permutation tests for investigating between-group differences showed decreased NWCP between SCN and FPN and DMN, which was accordant in BOLD and neural calculation. Besides, BOLD and neural also revealed specific alterations between networks (Fig. 6).

Taking the anatomic connections into consideration in studying the association between static and dynamic FC, the results of multi-regression analysis were illustrated in Supplementary material Fig. S5. Both the HC and GE showed negative regression coefficients of sFC in short-range connections (most intrahemispheric and a few interhemispheric). This negative association was consistent with the findings of partial correlation revealed above.

Discussion

The present study investigated the profiles of SC, sFC and dFC in patients with GE. Specifically, the sFC and dFC were calculated using both BOLD and neural time course. Besides, the association relationship between sFC and dFC was studied using partial correlation and GLM approaches. The present study revealed disrupted anatomical and functional profiles of DMN and primary networks, which was inferred to be responsible for epileptogenesis. Besides, predominantly disturbed

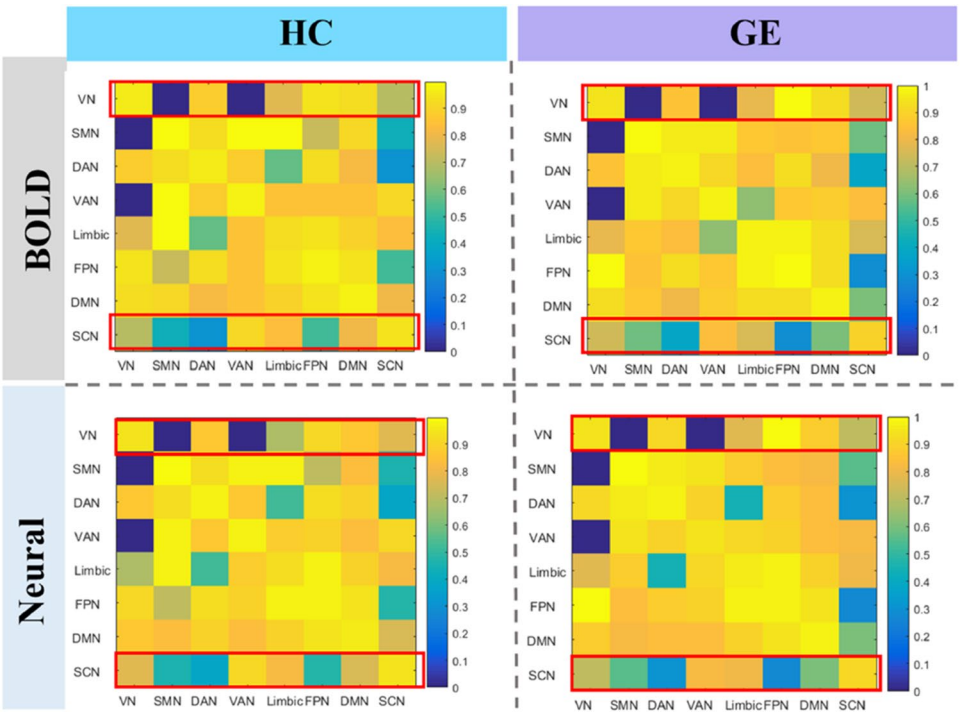

Fig. 5 Network-level of NWCP pattern in HC and GE. Except for relative low NWCP in VN- and SCN-related between-network connections, both groups showed concordant high NWCP values within and between networks

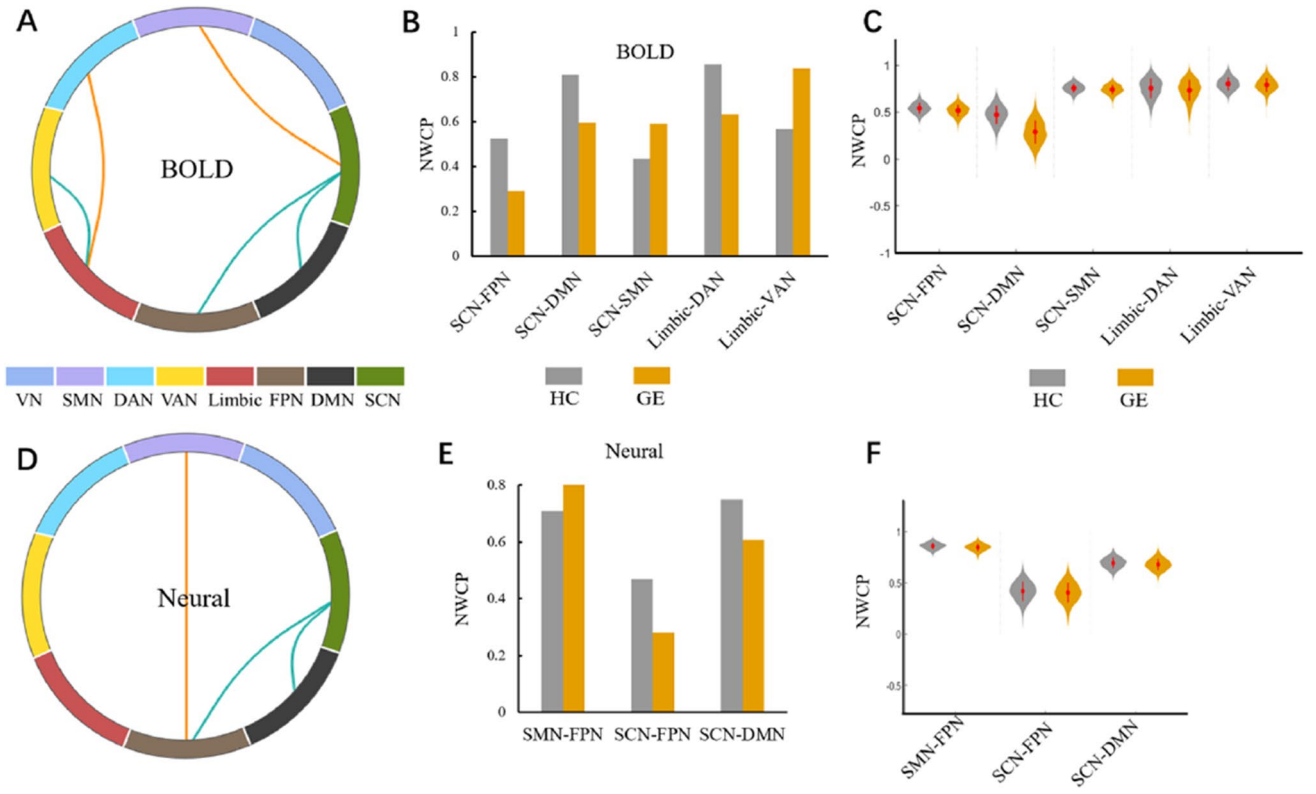

Fig. 6 Between-group differences of NWCP. Consistent alterations of NWCP were observed in the connections between SCN and FPN and DMN in BOLD (**a** and **b**) and neural time course-derived approaches (**d** and **e**). Besides, the distribution of the NWCP in HC and patients in permutations was presented using the violin plot (**c** and **f**)

connectivity between SCN and high-level networks provided evidence to help understand the modulation effects on epileptic activities and cognitive dysfunctions of patients. Moreover, negative correlation between dFC and sFC was demonstrated to be a common phenomenon in large-scale brain networks, reflecting the antagonistic relationship between stability and variability of brain. Decreased dFC-sFC association in SCN-DMN, and SCN-FPN implied an imbalance between stability and variability in GE, indicating a specific interaction pattern among core epileptic networks. The present finding provided a novel view to understand the pathological mechanism of epilepsy.

Notably, both the BOLD and neural analyses showed highly concordant results, even though preserving certain distinctions, respectively, which added powerful authenticity to the findings revealed in the present study. A summary integrating the concordant findings in core epileptic network in two approaches is illustrated in Fig. 7.

Epileptogenic brain characterized by connective profiles of DMN and primary networks

As known, the action of DMN is suspended during epileptic discharge period and is recognized to participate the

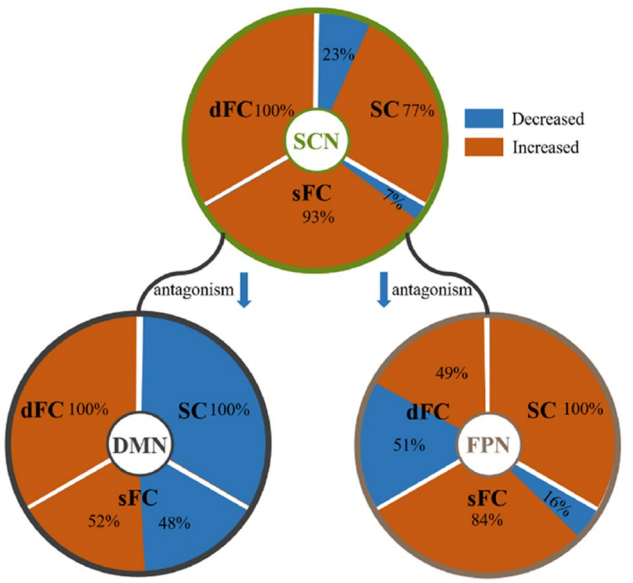

Fig. 7 Conclusion for the disturbed connective profiles and antagonism between dynamic and static connectivity in core networks in GE. The percentage in the figure represents the ratio of the number of increased or decreased connections to the total number of altered connections in patients with GE. The blue downward arrow represents decreased antagonism between networks

generation of generalized epileptic activities (Gotman et al. 2005; Richardson 2012). Accumulated studies have revealed disrupted internal functional integration and external functional interaction of DMN in patients with GE (Luo et al. 2011; Wei et al. 2015). In a word, the DMN has been identified to have a central role in epileptogenesis. For the connective profiles within the DMN, the present findings reveled disturbed functional integration and hypervariability in GE, providing clues to view the epileptogenic role of DMN. Cortical hyperexcitability is a significant signature for epileptogenesis and has been supposed to be related with dynamics features (Badawy et al. 2007; Hutchison et al. 2013a; Toth et al. 2018; Pawley et al. 2017). Hypervariability of FC within DMN potentially keeps in line with the hyperexcitability view and might contribute to the metastability of epileptic brain.

Primary brain dysfunction is a common phenomenon in GE, such as motor abnormality, visual aura, photosensitivity, and so on (Groppa et al. 2008; Bartolini et al. 2014). Actually, accumulated neuroimaging evidences have suggested abnormal connectivity of primary networks in common epilepsies (Wang et al. 2011; Cao et al. 2014). Decreased anatomical and functional connectivity within SMN observed in the present study implied insufficient information integration in patients with GE. Besides, internal hypervariability of SMN further implied a vulnerable state potentially corresponding to the motor abnormality. The photosensitivity and visual aura indicated potential disturbance of visual information processing in GE (Strigaro et al. 2012). Cautiously noted here, internal over-integration of VN might be associated with the visual symptoms of patients with GE (Brigo et al. 2013).

The DMN is responsible for internal spontaneous activities and primary networks take charge of the most basic information process from external stimulus, which plays the most important role for maintaining the fundamental state of brain. In the present study, abnormal connective profiles between DMN and primary networks were revealed in patients with GE. For the DMN, missing anatomic links with primary networks, stronger functional interactions with SMN, and weaker connectivity with VN were observed, which suggested disturbed information communication between DMN and primary networks. The decreased SC between DMN and SMN implied a possible anatomic pathway involved in the propagation of epileptic activities and deteriorated with the recurrent seizures. Moreover, on one hand, the over-interaction between DMN and SMN might be related with motor abnormality during seizures, on the other hand, it might create a condition more conducive to epileptogenesis in turn. Besides, attenuated static interaction and hypervariability of connectivity between DMN and VN were also observed in the present study. As demonstrated in the present findings, the SMN and VN demonstrated different connective profiles with DMN, suggesting specific involvement in GE.

Modulation role of SCN in the epileptic brain

In recent years, the SCN was widely recognized to be an effective modulator on epileptic activities (Luo et al. 2012; Vuong and Devergnas 2018; Miyamoto et al. 2019). The modulation effect of SCN is mainly realized by regulating the information interaction pattern between the cerebral networks directly or indirectly (Szaflarski et al. 2010). The thalamus and basal ganglia are the two most important subcortical regions. There is no doubt that the thalamus is a core region in the thalamocortical circuit in GE and widely and complexly connects with cerebral cortex during distinct epileptic actions (Gotman et al. 2005; Mishra et al. 2011; Jiang et al. 2018). Physiological and biochemical studies have indicated that the basal ganglia regulates the excitation and inhibition level of the cerebral cortex through the GABA system, which may be an important way to regulate the epileptic activities (Deransart et al. 1998; Chen et al. 2015). It has been suggested that striatum-modulated thalamocortical communication was associated with the susceptibility to secondary seizure generalization across multi brain networks (He et al. 2020). Besides, previous large-scale structural network analysis revealed disrupted topological organization of SCN in childhood absence epilepsy, suggesting an imperative focus on connective profiles of SCN in epilepsy (Xue et al. 2014). Consistently, the present work also revealed disturbed anatomic and functional connectivity between SCN and wide cerebral cortex, which further supported its high involvement in the long course of the disease. Specifically, stronger anatomical links and weaken functional interaction were observed in patients, implying that the SCN demonstrated a possible counter balance when communicating with epileptic networks. Moreover, the current work further provided evidence to suggest a state of hypervariability of SCN, which accords with its status as an engaged modulator in GE.

With long-term and recurrent seizures, the connective characteristics of SCN are proposed to be adaptively altered and contribute to corresponding individual behavior. In fact, except for responsible for epileptic activities, abnormal interaction between SCN and specific cortical regions was inferred to contribute to abnormal cognitive processing (Cerliani et al. 2015; Li et al. 2012). In GE, the SCN-modulated networks and the high-level networks overlapped significantly, thus the modulation of SCN on epileptic activities might disturb the activity of high-level networks and further affect the cognitive functions of patients. In the present study, it was found that the abnormal connectivity of the SCN was mainly connected to high-level networks. Weaker functional connectivity and hypervariability of interaction

between SCN and cognitive networks suggested an insufficient and unstable communication pattern in patients with GE, reflecting the potential effects of SCN on cognitive functions. Besides, reinforced anatomic connectivity in epilepsy is usually considered a compensation for decreased functional interaction (DeSalvo et al. 2014; Dong et al. 2016), which could partially interpret the stronger anatomic links observed in current study. In all, our findings provided a possible view to reveal the potential network mechanism of the modulation of SCN on epileptic activities and cognitive functions.

Even though there is no cognitive assessment in this work, previous studies have provided accumulated evidence suggesting cognitive impairment in GE (Chowdhury et al. 2014; Abarrategui et al. 2018). A previous study revealed that the altered connectivity between motor cortex and prefrontal cognitive cortex might be the underlying mechanism of cognition-induced motor abnormalities (Vollmar et al. 2012). In the present study, abnormal interaction between high-level and primary networks suggested abnormal integration and separation of information flow in patients with GE. Besides, hypovariability of functional interaction between high-level networks indicated inflexible communication, which might also be responsible for the cognitive dysfunction.

Disturbed antagonism between dynamic and static FC in core epileptic networks

In the present study, the antagonism effect between dynamic and static FC was significantly revealed in the HC group. It was found that the dFC is negatively correlated to sFC, that is, the stronger sFC is, the less dynamic it is. The stronger the sFC between two regions, the greater the probability that they will be the same functional module. Previous studies have found that the sFC within the same module is high, while the dynamics of connections within the same module is very low (Hutchison et al. 2013b). Besides, the functional connections within the rich club exhibit great stability and the variability of connections between nodes in rich club and other non-rich clubs is usually high (Shen et al. 2015). The low variability within modules is mainly to maintain the internal information integration of a cohesive functional system, while the high variability between modules corresponds to the flexible communication between multiple functional brain networks (Zalesky et al. 2014). These collective findings implied that the dFC shows a weakening trend with the increase of sFC strength, which is consistent with our current findings. The essence of dFC is the spontaneous alternation appearance of multi-stable patterns in accordance with certain rules, while sFC is the average performance of multiple states across complex spatio-temporal phenomena (Hutchison et al. 2013c; Allen et al. 2014; Preti et al. 2017). The preservation of antagonistic effects only in intrahemishereic short-range connections after regressing out the SC indicated the support role of the anatomic links in long-range connections. A previous study also revealed that longer range functional connections of the brain tend to be more dependent on structural connections (Shen et al. 2015). Stability and variability are two distinct aspects of functional interaction, reflected by the sFC and dFC, and mutual support and restraint each other. The balance of the level of dFC and sFC should be important for maintaining the stability and variability of brain.

In patients with GE, as discussed above, the DMN is recognized as a network involved in epileptic generation and propagation (Dong et al. 2016; Gotman 2008b). During the generalization, the thalamus played a crucial role in amplifying epileptic activities and spreading it to broader cerebral cortex (Gotman et al. 2005; Jiang et al. 2018), forming the well-known thalamocortical circuit responsible for underlying pathomechanism of GE. Using a 1 year of follow-up study, Wang et al. have revealed that the connective profiles in the thalamocortical loop is distinct in drug-resistant and seizure-free patients (Wang et al. 2019). Another structure of SCN, the basal ganglia has been recognized to present a potential modulation effect on epileptic actions (Loddenkemper et al. 2001; Miyamoto et al. 2019; Vuong and Devergnas 2018). It is worth noting that the FPN is one of the most frequently involved networks in epilepsy (Gotman 2008a; Laufs 2012; Carney et al. 2012). In the study of Wang et al., it also suggested that frontocentral networks might play a relay role in propagating abnormal activities to extended territories. Besides, marked thalamocortical imbalances was implied to contribute to the development of the disease. Specifically, the angular gyrus (an important node of the DMN) was involved in the imbalance. In the present study, the decreased dFC-sFC association in SCN-DMN and SCN-FPN implied imbalance of stability and variability, which might be the potential cause or result of the intrinsic epileptic state characterized by the imbalance of excitation and inhibition. We further speculated this alteration might be a crucial brain functional feature to reflect the specific interaction pattern among epileptogenesis, propagation, and modulation networks. An epileptic brain system composed of DMN, SCN and FPN was prudently proposed here trying to illustrate the network mechanism underlying generation, propagation and modulation of epileptic activities. In a word, our findings provide new clues to understand the pathomechanism of epilepsy from the abnormal association between dFC and sFC, which might be a useful indicator to investigate the pathomechanism underlying epilepsy.

Limitations

Using the BOLD and neural connectivity approaches to investigate the functional connective profiles in patients with GE, our work mainly focused on the consistent

findings revealed by two of them. Although the two methods reveal similar results to a large extent, there are some differences between BOLD and neural time course-derived connectivity, which could be partially explained by the variability of HRF from a notion in a previous study (Rangaprakash et al. 2018b). Because of the methodological limitations of blind deconvolution, to avoid excessive inference, the present study did not discuss the distinct findings of two approaches. The difference between BOLD and neural connectivity might imply some specific and meaningful information in epilepsy, which needs to be elucidated in future studies.

Conclusion

In summary, using BOLD and neural time course-derived methods, the patients with GE showed disturbed functional and structural connectivity predominately in DMN- and SCN-related connections, involving primary and high-level networks. Besides, antagonism (negative correlation) between dFC and sFC was identified as a common phenomenon in the large-scale network. Decreased antagonism between dFC and sFC in the connections between DMN and SCN, FPN implied imbalanced stability and variability in epileptogenesis, propagation, and modulation networks. The present study suggested that the coupling relationship between dFC and sFC might be a potential indicator to characterize functional abnormality related with epileptic actions.

Supplementary Information The online version contains supplementary material available at https://doi.org/10.1007/s00429-021-02248-1.

Acknowledgements The authors thank Professor Xiaoming Wang in the Affiliated Hospital of North Sichuan Medical College for their clinical support in the present study.

Funding This work was supported by the grant from National Key R&D Program of China (2018YFA0701400), the National Nature Science Foundation of China (U2033217, 61933003, 81960249 and 81771822), the PCSIRT project (IRT0910), and the CAMS Innovation Fund for Medical Sciences(CIFMS) (No. 2019-I2M-5–039).

Compliance with ethical standards

Conflict of interest The authors declare that they have no conflict of interest.

Ethical approval All procedures performed in studies involving human participants were approved by the ethical committee of the University of Electronic Science and Technology of China according to the standards of the Declaration of Helsinki.

Informed consent All participants provided written consent.

References

Abarrategui B, Parejo-Carbonell B, Garcia MEG, Di Capua D, Garcia-Morales I (2018) The cognitive phenotype of idiopathic generalized epilepsy. Epilepsy Behav 89:99–104. https://doi.org/10.1016/j.yebeh.2018.10.007

Allen EA, Damaraju E, Plis SM, Erhardt EB, Eichele T, Calhoun VD (2014) Tracking whole-brain connectivity dynamics in the resting state. Cereb Cortex 24(3):663–676. https://doi.org/10.1093/cercor/bhs352

Badawy RA, Curatolo JM, Newton M, Berkovic SF, Macdonell RA (2007) Changes in cortical excitability differentiate generalized and focal epilepsy. Ann Neurol 61(4):324–331. https://doi.org/10.1002/ana.21087

Bartolini E, Pesaresi I, Fabbri S, Cecchi P, Giorgi FS, Sartucci F, Bonuccelli U, Cosottini M (2014) Abnormal response to photic stimulation in Juvenile Myoclonic Epilepsy: An EEG-fMRI study. Epilepsia 55(7):1038–1047. https://doi.org/10.1111/epi.12634

Biswal B, Yetkin FZ, Haughton VM, Hyde JS (1995) Functional connectivity in the motor cortex of resting human brain using echo-planar Mri. Magn Reson Med 34(4):537–541. https://doi.org/10.1002/mrm.1910340409

Brigo F, Bongiovanni LG, Nardone R, Trinka E, Tezzon F, Fiaschi A, Manganotti P (2013) Visual cortex hyperexcitability in idiopathic generalized epilepsies with photosensitivity: a TMS pilot study. Epilepsy Behav 27(2):301–306. https://doi.org/10.1016/j.yebeh.2013.02.010

Cao XZ, Qian ZY, Xu Q, Shen JS, Zhang ZQ, Lu GM (2014) Altered intrinsic connectivity networks in frontal lobe epilepsy: a Resting-State fMRI Study. Comput Math Methods Med. https://doi.org/10.1155/2014/864979

Carney PW, Masterton RA, Flanagan D, Berkovic SF, Jackson GD (2012) The frontal lobe in absence epilepsy: EEG-fMRI findings. Neurology 78(15):1157–1165. https://doi.org/10.1212/WNL.0b013e31824f801d

Cerliani L, Mennes M, Thomas RM, Di Martino A, Thioux M, Keysers C (2015) Increased functional connectivity between subcortical and cortical resting-state networks in autism spectrum disorder. Jama Psychiat 72(8):767–777. https://doi.org/10.1001/jamapsychiatry.2015.0101

Chang C, Glover GH (2010) Time-frequency dynamics of resting-state brain connectivity measured with fMRI. Neuroimage 50(1):81–98. https://doi.org/10.1016/j.neuroimage.2009.12.011

Chen MM, Guo DQ, Li M, Ma T, Wu SD, Ma JL, Cui Y, Xia Y, Xu P, Yao DZ (2015) Critical roles of the direct GABAergic pallidocortical pathway in controlling absence seizures. PLoS Comp Biol 11(10):e1004539. https://doi.org/10.1371/journal.pcbi.1004539

Chowdhury FA, Elwes RDC, Koutroumanidis M, Morris RG, Nashef L, Richardson MP (2014) Impaired cognitive function in idiopathic generalized epilepsy and unaffected family members: an epilepsy endophenotype. Epilepsia 55(6):835–840. https://doi.org/10.1111/epi.12604

Deransart C, Vercueil L, Marescaux C, Depaulis A (1998) The role of basal ganglia in the control of generalized absence seizures. Epilepsy Res 32(1–2):213–223. https://doi.org/10.1016/S0920-1211(98)00053-9

DeSalvo MN, Douw L, Tanaka N, Reinsberger C, Stufflebeam SM (2014) Altered structural connectome in temporal lobe epilepsy. Radiology 270(3):842–848. https://doi.org/10.1148/radiol.13131044

Dong L, Luo C, Zhu Y, Hou C, Jiang S, Wang P, Biswal BB, Yao D (2016) Complex discharge-affecting networks in juvenile myoclonic epilepsy: a simultaneous EEG-fMRI study. Hum Brain Mapp 37(10):3515–3529. https://doi.org/10.1002/hbm.23256

Engel J, Jr., International League Against E (2001) A proposed diagnostic scheme for people with epileptic seizures and with epilepsy: report of the ILAE Task Force on Classification and Terminology. Epilepsia 42(6):796–803

Fan LZ, Li H, Zhuo JJ, Zhang Y, Wang JJ, Chen LF, Yang ZY, Chu CY, Xie SM, Laird AR, Fox PT, Eickhoff SB, Yu CS, Jiang TZ (2016) The human brainnetome atlas: a new brain atlas based on connectional architecture. Cereb Cortex 26(8):3508–3526. https://doi.org/10.1093/cercor/bhw157

Gotman J (2008a) Epileptic networks studied with EEG-fMRI. Epilepsia 49(Suppl 3):42–51. https://doi.org/10.1111/j.1528-1167.2008.01509.x

Gotman J (2008b) Epileptic networks studied with EEG-fMRI. Epilepsia 49:42–51. https://doi.org/10.1111/j.1528-1167.2008.01509.x

Gotman J, Grova C, Bagshaw A, Kobayashi E, Aghakhani Y, Dubeau F (2005) Generalized epileptic discharges show thalamocortical activation and suspension of the default state of the brain. Proc Natl Acad Sci USA 102(42):15236–15240. https://doi.org/10.1073/pnas.0504935102

Groppa S, Siebner HR, Kurth C, Stephani U, Siniatchkin M (2008) Abnormal response of motor cortex to photic stimulation in idiopathic generalized epilepsy. Epilepsia 49(12):2022–2029. https://doi.org/10.1111/j.1528-1167.2008.01709.x

He XS, Chaitanya G, Asma B, Caciagli L, Bassett DS, Tracy JI, Sperling MR (2020) Disrupted basal ganglia-thalamocortical loops in focal to bilateral tonic-clonic seizures. Brain 143:175–190. https://doi.org/10.1093/brain/awz361

Hutchison RM, Womelsdorf T, Allen EA, Bandettini PA, Calhoun VD, Corbetta M, Della Penna S, Duyn JH, Glover GH, Gonzalez-Castillo J, Handwerker DA, Keilholz S, Kiviniemi V, Leopold DA, de Pasquale F, Sporns O, Walter M, Chang C (2013a) Dynamic functional connectivity: promise, issues, and interpretations. Neuroimage 80:360–378. https://doi.org/10.1016/j.neuroimage.2013.05.079

Hutchison RM, Womelsdorf T, Allen EA, Bandettini PA, Calhoun VD, Corbetta M, Penna S, Duyn JH, Glover GH, Gonzalez-Castillo J, Handwerker DA, Keilholz S, Kiviniemi V, Leopold DA, Pasquale F, Sporns O, Walter M, Chang C (2013b) Dynamic functional connectivity: promise, issues, and interpretations. Neuroimage 80:360–378. https://doi.org/10.1016/j.neuroimage.2013.05.079

Hutchison RM, Womelsdorf T, Gati JS, Everling S, Menon RS (2013c) Resting-state networks show dynamic functional connectivity in awake humans and anesthetized macaques. Hum Brain Mapp 34(9):2154–2177. https://doi.org/10.1002/hbm.22058

Jiang S, Luo C, Gong J, Peng R, Ma S, Tan S, Ye G, Dong L, Yao D (2018) Aberrant thalamocortical connectivity in juvenile myoclonic epilepsy. IJNS 28(1):1750034. https://doi.org/10.1142/S0129065717500344

Kramer MA, Kolaczyk ED, Kirsch HE (2008) Emergent network topology at seizure onset in humans. Epilepsy Res 79(2–3):173–186. https://doi.org/10.1016/j.eplepsyres.2008.02.002

Laufs H (2012) Functional imaging of seizures and epilepsy: evolution from zones to networks. Curr Opin Neurol 25(2):194–200. https://doi.org/10.1097/WCO.0b013e3283515db9

Leonardi N, Van De Ville D (2015) On spurious and real fluctuations of dynamic functional connectivity during rest. Neuroimage 104:464–465. https://doi.org/10.1016/j.neuroimage.2014.10.045

Li YY, Wang JH, Jia LF, Zhao ZL, Lu J, Li KC, Jia JP, He Y, Jiang CL, Han Y (2012) Structural and functional Changes in subcortical vascular mild cognitive impairment: a combined voxel-based morphometry and Resting-State fMRI Study. PLoS ONE 7(9):e44758. https://doi.org/10.1371/journal.pone.0044758

Liu F, Wang YF, Li ML, Wang WQ, Li R, Zhang ZQ, Lu GM, Chen HF (2017) Dynamic functional network connectivity in idiopathic generalized epilepsy with generalized tonic-clonic seizure. Hum Brain Mapp 38(2):957–973. https://doi.org/10.1002/hbm.23430

Loddenkemper T, Pan A, Neme S, Baker KB, Rezai AR, Dinner DS, Montgomery EB Jr, Luders HO (2001) Deep brain stimulation in epilepsy. J Clin Neurophysiol 18(6):514–532

Lowe MJ, Dzemidzic M, Lurito JT, Mathews VP, Phillips MD (2000) Correlations in low-frequency BOLD fluctuations reflect cortico-cortical connections. Neuroimage 12(5):582–587. https://doi.org/10.1006/nimg.2000.0654

Luo C, Li QF, Lai YX, Xia Y, Qin Y, Liao W, Li SS, Zhou D, Yao DZ, Gong QY (2011) Altered functional connectivity in default mode network in absence epilepsy: a Resting-State fMRI Study. Hum Brain Mapp 32(3):438–449. https://doi.org/10.1002/hbm.21034

Luo C, Li QF, Xia Y, Lei X, Xue KQ, Yao ZP, Lai YX, Martinez-Montes E, Liao W, Zhou D, Valdes-Sosa PA, Gong QY, Yao DZ (2012) Resting state basal ganglia network in idiopathic generalized epilepsy. Hum Brain Mapp 33(6):1279–1294. https://doi.org/10.1002/hbm.21286

Mishra AM, Ellens DJ, Schridde U, Motelow JE, Purcaro MJ, DeSalvo MN, Enev M, Sanganahalli BG, Hyder F, Blumenfeld H (2011) Where fMRI and electrophysiology agree to disagree: corticothalamic and striatal activity patterns in the WAG/Rij rat. J Neurosci 31(42):15053–15064. https://doi.org/10.1523/JNEUROSCI.0101-11.2011

Miyamoto H, Tatsukawa T, Shimohata A, Yamagata T, Suzuki T, Amano K, Mazaki E, Raveau M, Ogiwara I, Oba-Asaka A, Hensch TK, Itohara S, Sakimura K, Kobayashi K, Kobayashi K, Yamakawa K (2019) Impaired cortico-striatal excitatory transmission triggers epilepsy. Nat Commun. 10:1917. https://doi.org/10.1038/S41467-019-09954-9

Mori S, van Zijl PCM (2002) Fiber tracking: principles and strategies-a technical review. NMR Biomed 15(7–8):468–480. https://doi.org/10.1002/nbm.781

Pawley AD, Chowdhury FA, Tangwiriyasakul C, Ceronie B, Elwes RDC, Nashef L, Richardson MP (2017) Cortical excitability correlates with seizure control and epilepsy duration in chronic epilepsy. Ann Clin Trans Neurol 4(2):87–97. https://doi.org/10.1002/acn3.383

Ponten SC, Bartolomei F, Stam CJ (2007) Small-world networks and epilepsy: graph theoretical analysis of intracerebrally recorded mesial temporal lobe seizures. Clin Neurophysiol 118(4):918–927. https://doi.org/10.1016/j.clinph.2006.12.002

Power JD, Barnes KA, Snyder AZ, Schlaggar BL, Petersen SE (2012) Spurious but systematic correlations in functional connectivity MRI networks arise from subject motion (vol 59, pg 2142, 2012). Neuroimage 63(2):999–999. https://doi.org/10.1016/j.neuroimage.2012.01.069

Preti MG, Bolton TAW, Van De Ville D (2017) The dynamic functional connectome: state-of-the-art and perspectives. Neuroimage 160:41–54. https://doi.org/10.1016/j.neuroimage.2016.12.061

Rangaprakash D, Deshpande G, Daniel TA, Goodman AM, Robinson JL, Salibi N, Katz JS, Denney TS, Dretsch MN (2017a) Compromised hippocampus-striatum pathway as a potential imaging biomarker of mild-traumatic brain injury and posttraumatic stress disorder. Hum Brain Mapp 38(6):2843–2864. https://doi.org/10.1002/hbm.23551

Rangaprakash D, Dretsch MN, Yan WJ, Katz JS, Denney TS, Deshpande G (2017b) Hemodynamic variability in soldiers with trauma: implications for functional MRI connectivity studies. Neuroimage-Clin 16:409–417. https://doi.org/10.1016/j.nicl.2017.07.016

Rangaprakash D, Dretsch MN, Venkataraman A, Katz JS, Denney TS, Deshpande G (2018a) Identifying disease foci from static and dynamic effective connectivity networks: illustration in soldiers with trauma. Hum Brain Mapp 39(1):264–287. https://doi.org/10.1002/hbm.23841

Rangaprakash D, Wu GR, Marinazzo D, Hu XP, Deshpande G (2018b) Hemodynamic response function (HRF) variability confounds

resting-state fMRI functional connectivity. Magn Reson Med 80(4):1697–1713. https://doi.org/10.1002/mrm.27146
Richardson MP (2012) Large scale brain models of epilepsy: dynamics meets connectomics. J Neurol Neurosur Ps 83(12):1238–1248. https://doi.org/10.1136/jnnp-2011-301944
Rubinov M, Sporns O (2011) Weight-conserving characterization of complex functional brain networks. Neuroimage 56(4):2068–2079. https://doi.org/10.1016/j.neuroimage.2011.03.069
Sakoglu U, Pearlson GD, Kiehl KA, Wang YM, Michael AM, Calhoun VD (2010) A method for evaluating dynamic functional network connectivity and task-modulation: application to schizophrenia. MRMPB 23(5–6):351–366. https://doi.org/10.1007/s10334-010-0197-8
Schindler KA, Bialonski S, Horstmann MT, Elger CE, Lehnertz K (2008) Evolving functional network properties and synchronizability during human epileptic seizures. Chaos 18(3):033119. https://doi.org/10.1063/1.2966112
Shen K, Hutchison RM, Bezgin G, Everling S, McIntosh AR (2015) Network structure shapes spontaneous functional connectivity dynamics. J Neurosci 35(14):5579–5588. https://doi.org/10.1523/Jneurosci.4903-14.2015
Sporns O, Chialvo DR, Kaiser M, Hilgetag CC (2004) Organization, development and function of complex brain networks. Trends Cogn Sci 8(9):418–425. https://doi.org/10.1016/j.tics.2004.07.008
Strigaro G, Prandi P, Varrasi C, Monaco F, Cantello R (2012) Defective visual inhibition in photosensitive idiopathic generalized epilepsy. Epilepsia 53(4):695–704. https://doi.org/10.1111/j.1528-1167.2012.03411.x
Szaflarski JP, DiFrancesco M, Hirschauer T, Banks C, Privitera MD, Gotman J, Holland SK (2010) Cortical and subcortical contributions to absence seizure onset examined with EEG/fMRI. Epilepsy Behav 18(4):404–413. https://doi.org/10.1016/j.yebeh.2010.05.009
Tagliazucchi E, Balenzuela P, Fraiman D, Chialvo DR (2012) Criticality in large-scale brain fMRI dynamics unveiled by a novel point process analysis. Front Physiol 3:15. https://doi.org/10.3389/Fphys.2012.00015
Toth K, Hofer KT, Kandracs A, Entz L, Bago A, Eross L, Jordan Z, Nagy G, Solyom A, Fabo D, Ulbert I, Wittner L (2018) Hyperexcitability of the network contributes to synchronization processes in the human epileptic neocortex. J Physiol-London 596(2):317–342. https://doi.org/10.1113/JP275413
Vollmar C, O'Muircheartaigh J, Symms MR, Barker GJ, Thompson P, Kumari V, Stretton J, Duncan JS, Richardson MP, Koepp MJ (2012) Altered microstructural connectivity in juvenile myoclonic epilepsy: the missing link. Neurology 78(20):1555–1559. https://doi.org/10.1212/WNL.0b013e3182563b44
Vuong J, Devergnas A (2018) The role of the basal ganglia in the control of seizure. J Neural Transm 125(3):531–545. https://doi.org/10.1007/s00702-017-1768-x
Wang Z, Dai Z, Gong G, Zhou C, He Y (2015) Understanding structural-functional relationships in the human brain: a large-scale network perspective. Neuroscientist 21(3):290–305. https://doi.org/10.1177/1073858414537560
Wang Z, Lariviere S, Xu Q, Vos de Wael R, Hong SJ, Wang Z, Xu Y, Zhu B, Bernasconi N, Bernasconi A, Zhang B, Zhang Z, Bernhardt BC (2019) Community-informed connectomics of the thalamocortical system in generalized epilepsy. Neurology 93(11):e1112–e1122. https://doi.org/10.1212/WNL.0000000000008096
Wang ZG, Lu GM, Zhang ZQ, Zhong YA, Jiao Q, Zhang ZJ, Tan QF, Tian L, Chen GH, Liao W, Li K, Liu YJ (2011) Altered resting state networks in epileptic patients with generalized tonic-clonic seizures. Brain Res 1374:134–141. https://doi.org/10.1016/j.brainres.2010.12.034
Wei HL, An J, Zeng LL, Shen H, Qiu SJ, Hu DW (2015) Altered functional connectivity among default, attention, and control networks in idiopathic generalized epilepsy. Epilepsy Behav 46:118–125. https://doi.org/10.1016/j.yebeh.2015.03.031
Winkler AM, Ridgway GR, Webster MA, Smith SM, Nichols TE (2014) Permutation inference for the general linear model. Neuroimage 92:381–397. https://doi.org/10.1016/j.neuroimage.2014.01.060
Wu GR, Liao W, Stramaglia S, Ding JR, Chen HF, Marinazzo D (2013) A blind deconvolution approach to recover effective connectivity brain networks from resting state fMRI data. Med Image Anal 17(3):365–374. https://doi.org/10.1016/j.media.2013.01.003
Xue K, Luo C, Zhang D, Yang T, Li J, Gong D, Chen L, Medina YI, Gotman J, Zhou D, Yao D (2014) Diffusion tensor tractography reveals disrupted structural connectivity in childhood absence epilepsy. Epilepsy Res 108(1):125–138. https://doi.org/10.1016/j.eplepsyres.2013.10.002
Yeo BTT, Krienen FM, Sepulcre J, Sabuncu MR, Lashkari D, Hollinshead M, Roffman JL, Smoller JW, Zoller L, Polimeni JR, Fischl B, Liu HS, Buckner RL (2011) The organization of the human cerebral cortex estimated by intrinsic functional connectivity. J Neurophysiol 106(3):1125–1165. https://doi.org/10.1152/jn.00338.2011
Zalesky A, Breakspear M (2015) Towards a statistical test for functional connectivity dynamics. Neuroimage 114:466–470. https://doi.org/10.1016/j.neuroimage.2015.03.047
Zalesky A, Fornito A, Cocchi L, Gollo LL, Breakspear M (2014) Time-resolved resting-state brain networks. Proc Natl Acad Sci USA 111(28):10341–10346. https://doi.org/10.1073/pnas.1400181111
Zhang ZQ, Liao W, Chen HF, Mantini D, Ding JR, Xu Q, Wang ZG, Yuan CP, Chen GH, Jiao Q, Lu GM (2011) Altered functional-structural coupling of large-scale brain networks in idiopathic generalized epilepsy. Brain 134:2912–2928. https://doi.org/10.1093/brain/awr223